Heat Capacity and Thermodynamic Properties of Sulfonate-Containing Zwitterions†

Xiu-Mei Liu,‡ Jun-ning Zhao,§ Qing-Shan Liu,‡ Li-xian Sun,§ Zhi-Cheng Tan,*,‡,§ and Urs Welz-Biermann*,‡

China Ionic Liquid Laboratory, Dalian Institute of Chemical Physics, Chinese Academy of Sciences, Dalian 116023, China, and Thermochemistry Laboratory, Dalian Institute of Chemical Physics, Chinese Academy of Sciences, Dalian 116023, China

Two sulfonate-containing zwitterions, 1-methylimidazolium-3-propylsulfonate zwitterion ($MimC_3SO_3$, $C_7H_{12}N_2O_3S$; CAS 179863-07-1) and 1-methylimidazolium-3-butylsulfonate zwitterion ($MimC_4SO_3$, $C_8H_{14}N_2O_3S$; CAS 148019-49-2), were prepared, and the structures were characterized by ^1H NMR and ^{13}C NMR and ESI-MS. The thermodynamic properties are investigated through adiabatic calorimetry (AC), differential scanning calorimetry (DSC), and thermogravimetric (TG) analysis. The low-temperature heat capacity ($C_{p,m}$) of $MimC_3SO_3$ and $MimC_4SO_3$ was measured in the temperature range from (78 to 400) K with a high precision automated calorimeter. The thermodynamic functions $[H_T - H_{298.15}]$ and $[S_T - S_{298.15}]$ were calculated based on the heat capacity data in the range from (80 to 400) K with an interval of 5 K.

Introduction

Ionic liquids (ILs) have been revealed as green reaction media owing to their negligible volatility, excellent thermal stability, remarkable solubility, the variety of structures available, liquidity over a wide temperature range, and high inherent conductivities.[1,2] Current research fields are divided into three categories: (a) as neoteric solvents as environmentally benign reaction media,[3,4] (b) as catalysts for organic reactions,[5−7] (c) and as electrolyte solutions for lithium battery applications,[8,9] fuel cells,[10,11] solar cells,[12,13] and capacitors.[14,15]

SO_3H-functionalized ionic liquids offer a new possibility for developing environmentally friendly acid catalysts because they combine the advantages of liquid acids and solid acids, uniform acid sites, water and air stable, easily separated, and reusable. Davis and co-workers observed temperature-controlled liquid−solid separation by using an alkane sulfonic acid IL as solvent/catalyst for esterification.[16] Other advantages of SO_3H-functionalized ILs for esterification are the high conversion rate and selectivity.[17,18] The synthetic approach of SO_3H-functionalized ILs is as follows: in the first step, the neutral nucleophiles react with sultone to give zwitterions.[19] In the second step, the zwitterion is mixed with strong Brönsted acid to obtain SO_3H-functionalized ILs. Therefore, as a precursor, the physicochemical properties of zwitterions directly affect the nature of the final ionic liquids. Moreover, zwitterionic compounds have always been an important material in the field of electrochemical applications. The addition of zwitterions to lithium salt in batteries shows the highest ionic conductivity.[20] Zwitterionic compounds are especially designed and used to tether the anion and cation making up ionic liquids, preventing migration under the influence of an electric field. These effects were first reported by Ohno and co-workers,[10] using zwitterionic compounds for large enhancement of lithium-ion diffusivity in polyelectrolyte gels. In addition, the electrochemical stability and conductivity of a zwitterionic imidazolium compound can be further improved significantly by changing the structure as reported.[21−23] The relationships between the structure of zwitterions and their thermal properties and their ionic conductivity after adding alkali metal salts have been discussed elsewhere.[20]

Most scientists have focused on the preparation and testing of SO_3H-functionlized ILs and zwitterion−LiTFSI mixtures, while few researchers put their efforts on fundamental thermodynamic studies. The thermodynamic properties of the zwitterions, such as heat capacity $C_{p,m}$, glass transition temperature T_g, melting temperature T_m,[20] thermal decomposition temperature T_d, enthalpy, and entropy are important properties that reflect the structures and stabilities of these compounds but are rarely reported. In this paper, the thermal stability of two sulfonate-containing zwitterions 1-methylimidazolium-3-propylsulfonate zwitterion ($MimC_3SO_3$) and 1-methylimidazolium-3-butylsulfonate zwitterion ($MimC_4SO_3$) were examined by differential scanning calorimetry (DSC) and thermogravimetry (TG). The low-temperature heat capacity over the temperature range from (78 to 400) K was measured by an automated adiabatic calorimeter, and the thermodynamic functions $[H_T - H_{298.15}]$ and $[S_T - S_{298.15}]$ were calculated in the above range based on the heat capacity measurements.

Experimental Section

Materials. All solvents and chemicals were commercially available. *N*-Methylimidazole was purchased from Linhai Kaile Chemicals Co.; 1,3-propane sultone and 1,4-butane sultone were purchased from Wuhan Fengfan Chemicals Co.; and other chemicals were purchased from Guoyao Group. All chemicals were distilled before use in the synthesis process.

Preparation and Characterization of $MimC_3SO_3$ (1) and $MimC_4SO_3$ (2). 1-Methylimidazole was mixed with 1,3-propane sultone or 1,4-butane sultone and stirred at room temperature for 8 h (Scheme 1). After solidification of the mass, the product (zwitterion) was washed three times with diethyl ether and then dried under vacuum (373 K, 1.33 Pa) for 8 h.[16] The samples were recrystallized twice from methanol and then dried under vacuum (373 K, 1.33 Pa) for 8 h again. Melting temperatures

† Part of the "Sir John S. Rowlinson Festschrift".

* Corresponding authors. E-mail: tzc@dicp.ac.cn (Zhi-Cheng Tan) and uwb@dicp.ac.cn (Urs Welz-Biermann).
‡ China Ionic Liquid Laboratory.
§ Thermochemistry Laboratory.

10.1021/je100423n
Published on Web 09/07/2010

Scheme 1. Synthesis of Two Sulfonate-Containing Zwitterions

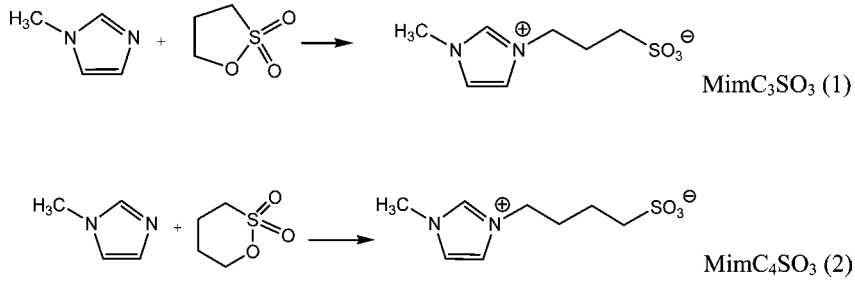

were determined using the Beijing Taike Melting point X-4 apparatus. The ^{1}H NMR and ^{13}C NMR spectra were recorded on a Bruker-400 MHz spectrometer. The molecular weight was determined by a UPLC/Q-Tof-mass spectrometer (UPLC/Q-Tof Micro). The compositions of two samples were determined with an Elemental Analyzer Vario EL III.

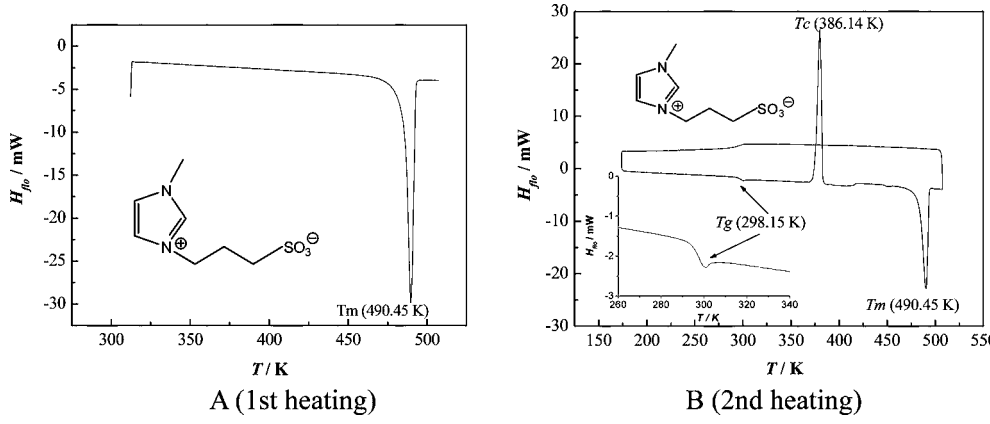

Figure 1. DSC curves of $MimC_3SO_3$. H_{flo} is the heat flow.

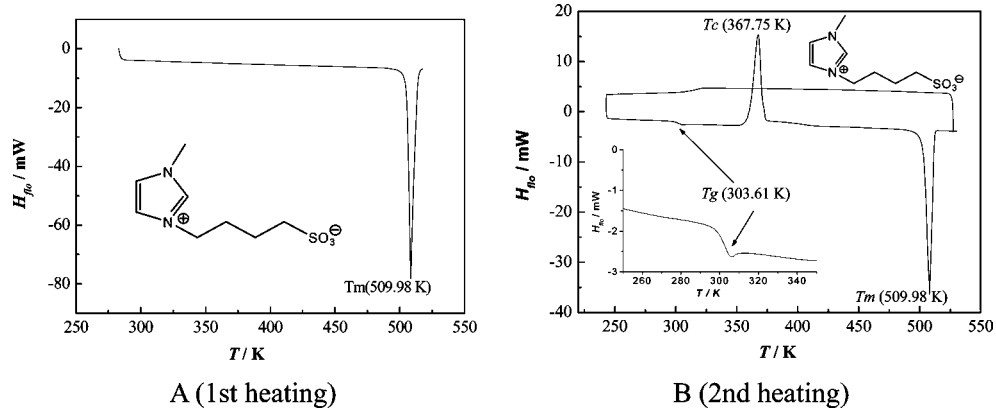

Figure 2. DSC curves of $MimC_4SO_3$. H_{flo} is the heat flow.

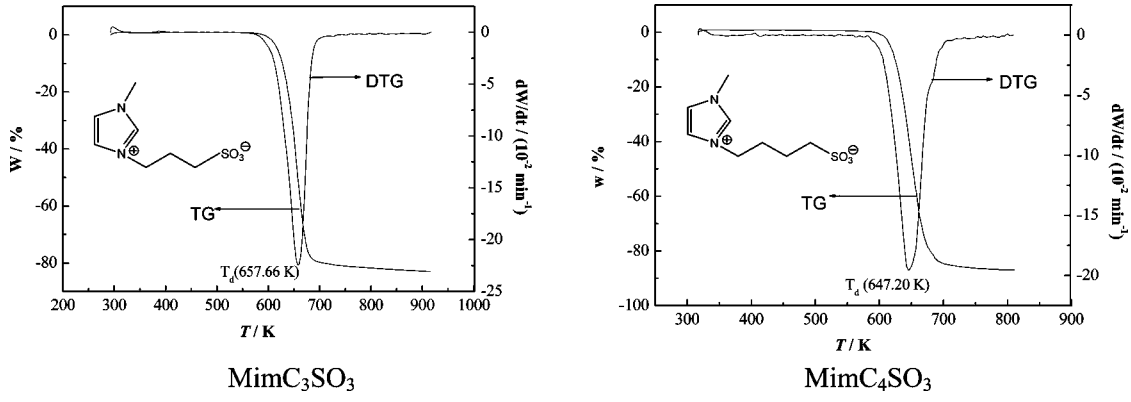

Figure 3. TG-DTG curves of $MimC_3SO_3$ and $MimC_4SO_3$under high purity nitrogen. *W* is the mass loss of the sample.

Table 1. Experimental Molar Heat Capacities of $MimC_3SO_3$ and $MimC_4SO_3$

T	$C_{p,m}$	T	$C_{p,m}$	T	$C_{p,m}$	T	$C_{p,m}$	T	$C_{p,m}$	T	$C_{p,m}$
K	$J\cdot K^{-1}\cdot mol^{-1}$	K	$J\cdot K^{-1}\cdot mol^{-1}$	K	$J\cdot K^{-1}\cdot mol^{-1}$	K	$J\cdot K^{-1}\cdot mol^{-1}$	K	$J\cdot K^{-1}\cdot mol^{-1}$	K	$J\cdot K^{-1}\cdot mol^{-1}$
					$MimC_3SO_3$						
79.798	86.51	185.77	156.95	293.53	222.83	133.585	127.13	239.79	186.01	345.86	260.16
81.816	88.12	187.72	158.74	295.51	223.55	135.532	131.14	242.05	187.95	347.69	257.32
83.716	89.95	189.66	159.79	297.50	224.52	137.523	130.24	244.34	187.83	349.60	262.66
85.644	89.73	191.59	160.39	299.48	225.32	139.481	129.74	246.29	188.35	351.56	261.97
87.557	93.20	193.51	162.15	301.46	225.86	141.427	131.92	248.25	190.30	353.54	259.52
89.487	95.76	195.43	163.86	303.43	227.02	143.368	134.51	250.19	193.13	355.49	263.89
91.402	97.65	197.40	164.54	305.40	226.03	145.334	134.71	252.14	194.47	357.41	266.15
93.323	99.15	199.41	165.47	307.36	230.37	147.339	135.23	254.07	195.68	359.38	268.15
95.238	102.59	201.87	167.03	309.31	235.18	149.318	136.30	255.99	196.30	361.39	270.90
97.168	103.14	204.26	168.03	311.27	235.45	151.859	137.15	257.92	197.35	363.37	269.56
99.118	102.97	206.21	169.73	313.22	236.03	154.342	136.69	259.83	198.68	365.32	267.19
101.851	103.15	208.23	170.72	315.16	234.76	156.255	139.22	261.74	199.57	367.26	270.08
104.552	104.71	210.24	171.01	317.10	236.03	158.240	141.20	263.64	200.05	369.16	275.79
106.455	105.28	212.24	172.70	319.02	238.01	160.198	143.21	265.55	201.61	371.10	275.40
108.386	105.70	214.24	173.59	320.95	239.81	162.157	143.46	267.43	202.34	373.06	275.42
110.330	111.76	216.23	174.98	322.87	240.52	164.101	142.79	269.32	203.12	375.00	277.14
112.289	111.65	218.22	175.65	324.78	243.51	166.030	143.55	271.30	205.52	376.96	279.35
114.183	111.92	220.20	176.48	326.69	246.23	167.953	145.47	273.27	206.92	378.97	280.38
116.128	115.43	222.16	177.33	328.59	244.95	169.862	147.40	275.24	208.19	380.96	281.24
118.099	116.28	224.13	178.37	330.48	246.48	171.838	148.97	277.30	209.38	383.24	283.27
120.052	114.78	226.09	179.05	332.37	249.83	173.855	149.72	279.36	210.92	385.55	285.76
121.970	115.61	228.04	180.76	334.35	249.15	175.864	149.26	281.42	212.37	387.47	284.60
123.876	119.92	229.98	181.37	336.32	251.01	177.862	149.24	283.48	214.25	389.43	285.05
125.819	122.24	231.89	182.01	338.27	250.40	179.850	152.16	285.52	216.30	391.54	286.70
127.786	123.43	233.91	183.89	340.28	254.40	181.845	150.39	287.56	218.37	393.53	288.42
129.739	125.12	235.92	184.74	342.23	256.80	183.803	154.14	289.55	220.99	395.46	290.84
131.673	124.91	237.85	185.76	344.09	255.82						
					$MimC_4SO_3$						
80.207	109.32	187.92	176.20	293.85	255.69	134.203	145.28	242.01	212.87	347.92	301.67
82.300	110.19	189.92	177.80	295.85	257.59	136.130	145.45	244.29	213.82	349.87	302.61
84.232	111.45	191.90	179.25	297.85	258.49	138.037	146.27	246.26	215.02	351.81	304.94
86.156	114.23	193.89	180.62	299.75	260.96	139.976	147.32	248.23	216.05	353.75	306.16
88.116	115.88	195.86	181.69	301.74	261.24	141.944	148.60	250.19	217.52	355.69	308.54
90.061	117.56	197.82	183.02	303.72	264.66	143.895	150.42	252.24	219.72	357.62	308.82
92.014	118.29	199.78	184.59	305.71	264.36	145.836	151.09	254.30	221.07	359.54	310.24
93.950	119.31	202.16	186.03	307.78	264.22	147.759	152.25	256.34	222.28	361.47	312.31
95.894	120.93	204.55	188.92	309.84	267.13	149.673	153.38	258.38	223.16	363.48	313.02
97.833	122.20	206.52	189.41	311.90	269.55	152.188	153.72	260.41	224.41	365.48	315.16
99.771	123.74	208.48	190.86	313.95	271.31	154.712	155.47	262.43	226.87	367.47	315.19
102.476	124.48	210.43	192.56	315.99	273.57	156.629	157.00	264.45	228.30	369.54	318.14
105.122	126.89	212.37	193.16	318.03	274.90	158.538	158.94	266.45	230.63	371.62	320.13
107.002	127.99	214.31	194.31	320.06	276.18	160.498	159.74	268.46	233.04	373.68	321.14
108.909	129.52	216.23	195.92	322.09	278.14	162.511	160.66	270.45	233.66	375.73	323.95
110.848	130.01	218.15	196.94	324.11	279.41	164.510	162.30	272.44	235.64	377.79	324.83
112.807	131.16	220.06	198.36	326.12	281.91	166.501	163.42	274.42	237.81	379.83	325.26
114.747	132.61	221.95	199.16	328.13	283.31	168.481	163.25	276.40	239.51	381.87	327.60
116.665	133.57	223.84	200.40	330.13	285.02	170.445	164.22	278.38	241.25	383.90	332.07
118.608	135.14	225.81	201.12	332.13	286.68	172.403	166.07	280.34	243.42	385.94	334.00
120.580	137.07	227.76	203.49	334.12	289.14	174.344	169.35	282.30	245.29	387.96	335.27
122.533	137.67	229.69	205.70	336.11	290.13	176.292	169.43	284.25	246.94	389.98	335.42
124.464	138.87	231.68	206.80	338.09	291.64	178.223	169.86	286.19	249.67	391.98	337.63
126.381	139.75	233.67	207.23	340.07	293.16	180.140	172.46	288.12	252.87	393.99	338.39
128.324	140.75	235.68	210.00	342.04	294.72	182.059	172.94	290.04	253.95	395.97	341.92
130.297	142.40	237.67	211.80	344.00	297.82	183.961	173.45	291.95	254.73	397.96	344.53
132.250	144.69	239.66	212.72	345.96	300.22	185.912	174.79				

The obtained data are in good agreement with those reported in the literature.[16,20] $MimC_3SO_3$: ^1H NMR (400 MHz, D_2O, TMS) δ (ppm) 2.317 (m, 2H), 2.921 (t, 2H), 3.894 (s, 3H), 4.365 (t, 2H), 7.447 (s, 1H), 7.524 (s, 1H), 8.757 (s, 1H); ^{13}C NMR (400 MHz, D_2O, TMS) δ (ppm) 24.549, 35.154, 46.648, 47.180, 121.647, 123.212, 135.664.

HRMS (ESI), m/z: $[M + Na]^+$ calcd for $C_7H_{12}N_2O_3NaS$, 227.0466; found, 227.0475. Elemental analytical calculation for $C_7H_{12}N_2O_3S$: C 41.2, H 5.94, N 13.73; found C 40.63, H 5.80, N 13.25. The purity was 98.8 %. Melting point, $T_m = 490$ K.

$MimC_4SO_3$: ^1H NMR (400 MHz, D_2O, TMS) δ (ppm) 1.756 (m, 2H), 2.039 (m, 2H), 2.954 (t, 2H), 3.906 (s, 3H), 4.263 (t, 2H), 7.455 (s, 1H), 7.515 (s, 1H), 8.756 (s, 1H); ^{13}C NMR (400 MHz, D_2O, TMS) δ (ppm) 20.405, 27.583, 35.137, 48.394, 49.539, 121.649, 123.135, 135.135.

HRMS (ESI), m/z: $[M + Na]^+$ calcd for $C_8H_{14}N_2O_3NaS$, 241.0623; found, 241.0627. Elemental analytical calculation for $C_8H_{14}N_2O_3S$: C 44.06, H 6.48, N 12.85; found C 43.66, H 6.73, N 12.16. The purity was 99.1 %. Melting point, $T_m = 509$ K.

Thermal Analysis. DSC analysis was carried out in a Netzsch differential scanning calorimeter (model: DSC 204) under N_2 with a flow rate of 25 mL·min^{-1}. The samples were first heated with a rate of 10 K·min^{-1} from room temperature to 550 K and then cooled with the same rate from (550 to 150) K and then heated with the same rate from (150 to 550) K. The sample (about 6.00 mg) was weighted into a aluminum pan, placed in the DSC cell, and heated at the rate of 10 K·min^{-1} under high purity nitrogen atmosphere with a flow rate of 25 mL·min^{-1}. Thermogravimetric (TG) measurement was performed on Setaram Setsys 16/18 apparatus. A mass of 5.68 mg was placed in a 100 μL α-alumina crucible and heated from room temperature to 500 K with a rate of 10 K·min^{-1} under high purity nitrogen atmosphere with a flow rate of 60 mL·min^{-1}.

Adiabatic Calorimetry (AC). Heat capacity measurements were carried out in a high-precision automated adiabatic calorimeter[24−26] which was established by the Thermochemistry Laboratory of Dalian Institute of Chemical Physics, Chinese Academy of Sciences, in PR China. To verify the reliability of the adiabatic calorimeter, the molar heat capacities for Standard Reference Material 720, Synthetic Sapphire (α-Al_2O_3), were measured. The deviations of our experimental results from the recommended values by NIST[27] were within ± 0.1 % in the temperature range from (78 to 400) K. The $MimC_3SO_3$ mass used for the heat capacity measurement was 3.25261 g, which is equivalent to 0.01594 mol based on the molar mass, M = 204.0475 g·mol^{-1}. The $MimC_4SO_3$ mass used for the heat capacity measurement was 3.32591 g which is equivalent to 0.01521 mol based on the molar mass, M = 218.0627 g·mol^{-1}. The temperature increment was 2 K in a heating period, and the drift of temperature was 10^{-4} K·min^{-1} for each experimental heat capacity point.

Results and Discussion

Thermal Properties and Phase Behavior of $MimC_3SO_3$ and $MimC_4SO_3$ Tested by DSC and TG. The phase behaviors of $MimC_3SO_3$ and $MimC_4SO_3$, such as freezing, melting, and glass transition, were studied with DSC. The results are summarized in Table 3. The DSC curves of $MimC_3SO_3$ and $MimC_4SO_3$ are shown in Figures 1 and 2. For $MimC_3SO_3$ in the first heating, only one melting process with a peak temperature of (490.45 ± 0.51) K was observed. In the second heating cycle, a glass transition temperature T_g, at (298.15 ± 0.32) K, a crystallization point T_c at (386.14 ± 0.41) K, and a melting point T_m at (490.45 ± 0.51) K were observed, which coincides with the literature values.[20] The molar enthalpy ($\Delta_{cry}H$) of crystallization was determined to be (−28.93 ± 0.29) kJ·mol^{-1} by integration of the area of the first peak. The molar entropy ($\Delta_{cry}S$) of crystallization was derived to be (−74.92 ± 0.75) J·K^{-1}·mol^{-1}. The molar enthalpy of fusion ($\Delta_{fus}H$) was determined to be (28.38 ± 0.28) kJ·mol^{-1} by integration of the area of the second peak. The molar entropy ($\Delta_{fus}S$) of fusion was derived to be (57.86 ± 0.58) J·K^{-1}·mol^{-1}.

Similarly, for $MimC_4SO_3$ in the first heating only one melting point at (508.98 ± 0.71) K occurred, and in the second heating a glass transition temperature T_g, crystallization point T_c, and melting point T_m were observed at (303.61 ± 0.56) K, (367.75 ± 0.62) K, and (509.98 ± 0.71) K, respectively. The molar enthalpy ($\Delta_{cry}H$) and entropy ($\Delta_{cry}S$) of crystallization were determined to be (−17.71 ± 0.18) kJ·mol^{-1} and (−48.15 ± 0.45) J·K^{-1}·mol^{-1} respectively. The molar enthalpy ($\Delta_{fus}H$) and entropy ($\Delta_{fus}S$) of fusion were determined to be (25.16 ± 0.21) kJ·mol^{-1} and (49.33 ± 0.47) J·K^{-1}·mol^{-1}, respectively.

From DSC curves of two samples, crystallization was observed in the second heating process, which means that the crystallization rates of sulfonate-containing zwitterions are very slow and that the supercooled liquids are fairly stable. An interesting phenomenon of supercooled liquid crystalline was also observed.

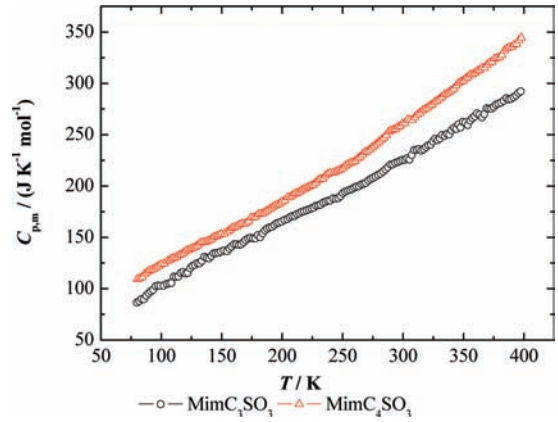

Figure 4. Experimental molar heat capacity $C_{p,m}$ as a function of temperature for $MimC_3SO_3$ and $MimC_4SO_3$ from (78 to 400) K.

Thermal Decomposition Temperature. The TG-DTG curves are shown in Figure 3. It can be seen that the mass loss of $MimC_3SO_3$ was completed in a single step. The sample keeps thermostable below 570 K. The weight loss begins at about 580 K, reaches the maximum rate of weight loss at (657.66 ± 0.58) K, and completes losing weight when the temperature reaches 710 K. A similar one-step decomposition process occurs for $MimC_4SO_3$ beginning at about 570 K and finishing at about 700 K, while the peak temperature of decomposition is (647.20 ± 0.65) K.

Low-Temperature Heat Capacity. The experimental molar heat capacities of $MimC_3SO_3$ and $MimC_4SO_3$ measured by the adiabatic calorimeter over the experimental temperature range are listed in Table 1 and plotted in Figure 4, respectively. The relative contribution of the sample to the total heat capacity including the sample vessel was 0.37 (80 K) and 0.48 (400 K).

For $MimC_3SO_3$, a smoothed curve with no endothermic or exothermic peaks was observed from the liquid nitrogen temperature to 400 K, which indicated that the sample is thermostable in this temperature range. The values of experimental heat capacities can be fitted to the following polynomial equations with the least-squares method:[27]

Before the fusion, T = (78 to 400) K

$$C_{p,m}/\mathrm{J\cdot K^{-1}\cdot mol^{-1}} = 186.443 + 93.108x + 20.358x^2 + 14.549x^3 - 22.457x^4 - 5.567x^5 + 5.047x^6$$

where x is the reduced temperature, $x = [T - (T_{max} + T_{min})/2]/[(T_{max} - T_{min})/2]$; T is the experimental temperature; and T_{max} and T_{min} are the upper and lower limit in the temperature region. The correlation coefficient of the fitting r^2 = 0.9994. The standard diveation in C_p is ± 0.3 %.

Similarly, for $MimC_4SO_3$ the values of experimental heat capacities were fitted to the following polynomial equations with the least-squares method:

Before the fusion, T = (78 to 400) K

$$C_{p,m}/\mathrm{J\cdot K^{-1}\cdot mol^{-1}} = 210.932 + 116.917x + 31.461x^2 - 4.939x^3 - 23.991x^4 - 4.687x^5 + 7.981x^6$$

Table 2. Smoothed Heat Capacities and Thermodynamic Functions of $MimC_3SO_3$ and $MimC_4SO_3$

T / K	$C_{p,m}$ / J·K^{-1}·mol^{-1}	$H_T - H_{298.15}$ / kJ·mol^{-1}	$S_T - S_{298.15}$ / J·K^{-1} mol^{-1}	$C_{p,m}$ / J·K^{-1} mol^{-1}	$H_T - H_{298.15}$ / kJ·mol^{-1}	$S_T - S_{298.15}$ / J·K^{-1} mol^{-1}
		$MimC_3SO_3$			$MimC_4SO_3$	
80	87.30	−34.40	−188.95	109.72	−39.24	−216.78
85	91.29	−33.96	−183.54	113.17	−38.68	−210.03
90	95.22	−33.49	−178.21	116.58	−38.11	−203.47
95	99.08	−33.01	−172.96	119.93	−37.52	−197.07
100	102.86	−32.50	−167.78	123.22	−36.91	−190.83
105	106.57	−31.98	−162.67	126.46	−36.29	−184.73
110	110.20	−31.44	−157.62	129.66	−35.65	−178.77
115	113.75	−30.88	−152.64	132.80	−34.99	−172.94
120	117.21	−30.30	−147.73	135.90	−34.32	−167.22
125	120.60	−29.70	−142.88	138.95	−33.63	−161.61
130	123.90	−29.09	−138.08	141.98	−32.93	−156.1
135	127.13	−28.47	−133.35	144.97	−32.21	−150.69
140	130.29	−27.82	−128.67	147.94	−31.48	−145.37
145	133.38	−27.16	−124.05	150.90	−30.73	−140.13
150	136.41	−26.49	−119.47	153.84	−29.97	−134.96
155	139.38	−25.80	−114.95	156.79	−29.19	−129.87
160	142.30	−25.09	−110.48	159.73	−28.40	−124.85
165	145.17	−24.38	−106.06	162.68	−27.60	−119.89
170	148.01	−23.64	−101.69	165.65	−26.78	−114.99
175	150.81	−22.90	−97.35	168.65	−25.94	−110.14
180	153.58	−22.13	−93.07	171.67	−25.09	−105.35
185	156.33	−21.36	−88.82	174.72	−24.22	−100.6
190	159.07	−20.57	−84.61	177.81	−23.34	−95.9
195	161.81	−19.77	−80.44	180.95	−22.44	−91.24
200	164.54	−18.95	−76.31	184.13	−21.53	−86.61
205	167.28	−18.12	−72.21	187.37	−20.60	−82.02
210	170.03	−17.28	−68.15	190.66	−19.66	−77.47
215	172.79	−16.42	−64.11	194.01	−18.70	−72.94
220	175.58	−15.55	−60.11	197.41	−17.72	−68.44
225	178.39	−14.67	−56.13	200.88	−16.72	−63.96
230	181.24	−13.77	−52.18	204.42	−15.71	−59.51
235	184.11	−12.85	−48.25	208.01	−14.68	−55.07
240	187.03	−11.93	−44.34	211.67	−13.63	−50.65
245	189.99	−10.98	−40.46	215.39	−12.56	−46.25
250	192.99	−10.03	−36.59	219.17	−11.47	−41.86
255	196.03	−9.05	−32.74	223.01	−10.37	−37.49
260	199.12	−8.07	−28.91	226.90	−9.24	−33.12
265	202.26	−7.06	−25.08	230.85	−8.10	−28.76
270	205.44	−6.04	−21.27	234.85	−6.94	−24.41
275	208.68	−5.01	−17.48	238.90	−5.75	−20.07
280	211.95	−3.96	−13.69	242.99	−4.55	−15.73
285	215.27	−2.89	−9.91	247.12	−3.32	−11.39
290	218.63	−1.80	−6.14	251.28	−2.08	−7.06
295	222.03	−0.70	−2.37	255.47	−0.81	−2.73
298.15	**224.19**	**0.00**	**0.00**	**258.12**	**0.00**	**0.00**
300	225.47	0.42	1.39	259.68	0.48	1.6
305	228.93	1.55	5.15	263.92	1.79	5.93
310	232.42	2.71	8.90	268.17	3.12	10.26
315	235.94	3.88	12.65	272.43	4.47	14.58
320	239.47	5.06	16.39	276.69	5.84	18.91
325	243.01	6.27	20.13	280.96	7.24	23.23
330	246.55	7.49	23.87	285.22	8.65	27.56
335	250.10	8.74	27.60	289.48	10.09	31.88
340	253.63	10.00	31.34	293.73	11.55	36.21
345	257.15	11.27	35.07	297.97	13.03	40.53
350	260.64	12.57	38.79	302.21	14.53	44.85
355	264.11	13.88	42.51	306.43	16.05	49.16
360	267.53	15.21	46.23	310.65	17.59	53.48
365	270.91	16.55	49.94	314.86	19.15	57.79
370	274.23	17.92	53.65	319.07	20.74	62.1
375	277.49	19.30	57.35	323.29	22.35	66.41
380	280.68	20.69	61.05	327.52	23.97	70.72
385	283.79	22.10	64.74	331.78	25.62	75.03
390	286.82	23.53	68.42	336.07	27.29	79.33
395	289.76	24.97	72.09	340.41	28.98	83.64

The correlation coefficient of the fitting is $r^2 = 0.9998$. The standard diveation in C_p is ± 0.3 %.

Thermodynamic Function. The thermodynamic functions ($H_T^0 - H_{298.15}^0$) and ($S_T^0 - S_{298.15}^0$) of the two sulfonate-containing zwitterions relative to the reference temperature 298.15 K were calculated in the experimental temperature range with an interval of 5 K, using the polynomial equations of heat capacity and thermodynamic relationships as follows:

For $MimC_3SO_3$, before melting

$$H_T^0 - H_{298.15}^0 = \int_{298.15}^{T} C_{p,m}^0(s)\mathrm{d}T$$

$$S_T^0 - S_{298.15}^0 = \int_{298.15}^{T} \frac{C_{p,m}^0(s)}{T}\mathrm{d}T$$

For $MimC_4SO_3$, the calculation of thermodynamic functions is the same as $MimC_3SO_3$ before and after the melting.

Table 3. Thermal Properties and Phase Behavior of Sulfonate-Containing Zwitterions

parameters	$MimC_3SO_3$	$MimC_4SO_3$	comparison
$C_{p,m(298.15)}$/J·K^{-1}·mol^{-1}	224.19 ± 0.67	252.12 ± 0.76	$C_{p,m}$: $MimC_3SO_3$ < $MimC_4SO_3$
$\Delta_{cry}H$/kJ·mol^{-1}	−28.93 ± 0.29	−17.71 ± 0.18	$\Delta_{cry}H$: $MimC_3SO_3$ < $MimC_4SO_3$
$\Delta_{cry}S$/J·K^{-1}·mol^{-1}	−74.92 ± 0.75	−48.15 ± 0.45	$\Delta_{cry}S$: $MimC_3SO_3$ < $MimC_4SO_3$
$\Delta_{fus}H$/kJ·mol^{-1}	28.38 ± 0.28	25.16 ± 0.21	$\Delta_{fus}H$: $MimC_3SO_3$ > $MimC_4SO_3$
$\Delta_{fus}S$/J·K^{-1}·mol^{-1}	57.86 ± 0.58	49.33 ± 0.47	$\Delta_{fus}S$: $MimC_3SO_3$ > $MimC_4SO_3$
T_g/K	298.15 ± 0.32	303.61 ± 0.56	T_g: $MimC_3SO_3$ < $MimC_4SO_3$
T_c/K	386.14 ± 0.41	367.75 ± 0.62	T_c: $MimC_3SO_3$ > $MimC_4SO_3$
T_m/K	490.45 ± 0.51	509.98 ± 0.71	T_m: $MimC_3SO_3$ < $MimC_4SO_3$
T_d/K	657.66 ± 0.58	647.20 ± 0.65	T_d: $MimC_3SO_3$ > $MimC_4SO_3$

The standard thermodynamic functions, $H_T^0 - H_{298.15}^0$ and $S_T^0 - S_{298.15}^0$, of the two sulfonate-containing zwitterions are listed in Table 2.

Comparison and Estimation of Thermodynamic Properties for Sulfonate-Containing Zwitterions. According to experimental data (Table 3), the thermodynamic properties as well as the structure of $MimC_3SO_3$ and $MimC_4SO_3$ were compared with each other and estimated as follows:

(a) Molar heat capacity $C_{p,m}$, molar crystallization enthalpy ΔH_{cry}, melting temperature T_m, glass transition temperature T_g: $MimC_3SO_3$ < $MimC_4SO_3$. Molar fusion enthalpy $\Delta_{fus}H$ and crystallization temperature T_c: $MimC_3SO_3$ > $MimC_4SO_3$. These data reveal that $MimC_3SO_3$ has lower lattice energy than $MimC_4SO_3$ at low temperature due to a shorter carbon chain in the structure of $MimC_3SO_3$. The difference of properties between two compounds can be rationalized as follows: (a) the molecular symmetry of $MimC_3SO_3$ is lower than $MimC_4SO_3$ and (b) the intermolecular interaction of $MimC_3SO_3$ is lower than $MimC_4SO_3$.

(b) The higher thermal decomposition temperature T_d of $MimC_3SO_3$ indicates an increased thermal stability due to a higher bond energy of the C−N bond in the structure of $MimC_3SO_3$.

Conclusions

Two sulfonate-containing zwitterions ($MimC_3SO_3$ and $MimC_4SO_3$) were prepared, and the structures were verified by ^{1}H NMR and ^{13}C NMR. Their thermodynamic properties were studied by adiabatic calorimetry (AC), differential scanning calorimetry (DSC), and thermogravimatric analysis (TG-DTG). The phase change behavior and thermodynamic properties of $MimC_3SO_3$ and $MimC_4SO_3$ were compared. Results indicate that $MimC_4SO_3$ has higher $\Delta_{cry}H$, T_m, and T_g and lower T_d, $\Delta_{fus}H$, and T_c than $MimC_3SO_3$ due to their different molecular structures. Low-temperature heat capacity ($C_{p,m}$) of $MimC_3SO_3$ and $MimC_4SO_3$ were measured in the temperature range from (78 to 400) K with a high precision automated adiabatic calorimeter (AC), and no phase transition or thermal anomaly was observed in this range, The thermodynamic functions ($H_T^0 - H_{298.15}^0$) and ($S_T^0 - S_{298.15}^0$) of the two sulfonate-containing zwitterions relative to the reference temperature 298.15 K were calculated.

Literature Cited

(1) Bates, E. D.; Mayton, R. D.; Ntai, I.; Davis, J. H., Jr. CO_2 Capture by a Task-Specific Ionic Liquid. *J. Am. Chem. Soc.* **2002**, *124*, 926–927.

(2) Visser, A. E.; Holbrey, J. D.; Rogers, R. D. Hydrophobic ionic liquids incorporating *N*-alkylisoquinolinium cations and their utilization in liquid-liquid separations. *Chem Commun.* **2001**, 2484–2485.

(3) Welton, T. Room-Temperature Ionic Liquids. Solvents for Synthesis and Catalysis. *Chem. Rev.* **1999**, *99*, 2071–2084.

(4) Wasserscheid, P.; Keim, W. Ionic Liquids - New "Solutions" for Transition Metal Catalysis. *Angew. Chem., Int. Ed.* **2000**, *39*, 3772–3789.

(5) Parvulescu, V. I.; Hardacre, C. Catalysis in ionic liquids. *Chem. Rev.* **2007**, *107*, 2615–2665.

(6) Ikegami, S.; Hamamoto, H. Novel Recycling System for Organic Synthesis via Designer Polymer-Gel Catalysts. *Chem. Rev.* **2009**, *109*, 583–593.

(7) Karout, A.; Pierre, A. C. Silica gelation catalysis by ionic liquids. *Catal. Commun.* **2009**, *10*, 359–361.

(8) Chagnes, A.; Diaw, M.; Carré, B.; Willmann, P.; Lemordant, D. Imidazolium-organic solvent mixtures as electrolytes for lithium batteries. *J. Power Sources* **2005**, *145* (1), 82–88.

(9) Hayashi, K.; Nemoto, Y.; Akuto, K.; Sakurai, Y. Alkylated imidazolium salt electrolyte for lithium cells. *J. Power Sources* **2005**, *146* (12), 689–692.

(10) Noda, A.; Susan, M.; Kudo, K.; Mitsushima, S.; Hayamizu, K.; Watanabe, M. Brønsted Acid-Base Ionic Liquids as Proton-Conducting Nonaqueous Electrolytes. *J. Phys. Chem. B* **2003**, *107* (17), 4024–4033.

(11) Susan, M.; Noda, A.; Mitsushima, S.; Watanabe, M. Brønsted acid-base ionic liquids and their use as new materials for anhydrous proton conductors. *Chem. Commun.* **2003**, 938–939.

(12) Haskouri, J.; Zárate, D. O.; Guillem, C.; Latorre, J.; Caldés, M.; Beltrán, A.; Beltrán, D.; Descalzo, A. B.; López, G. R.; Máñez, R. M.; Marcos, M. D.; Amorós, P. Silica-based powders and monoliths with bimodal pore systems. *Chem. Commun.* **2002**, 330–331.

(13) Kubo, W.; Kitamura, T.; Hanabusa, K.; Wada, Y.; Yanagida, S. Quasi-solid-state dye-sensitized solar cells using room temperature molten salts and a low molecular weight gelator. *Chem. Commun.* **2002**, 374–375.

(14) Rochefort, D.; Pont, A. L. Pseudocapacitive behaviour of RuO_2 in a proton exchange ionic liquid. *Electrochem. Commun.* **2006**, *8* (9), 1539–1543.

(15) Nagao, Y.; Nakayama, Y.; Oda, H.; Ishikawa, M. Activation of an ionic liquid electrolyte for electric double layer capacitors by addition of $BaTiO_3$ to carbon electrodes. *J. Power Sources* **2007**, *166* (2), 595–598.

(16) Amanda, C. C.; Jessica, L. J.; Ioanna, N.; Kim, L.T. T.; Kristin, J. W.; David, C. F.; James, H. D., Jr. Novel Brønsted Acidic Ionic Liquids and Their Use as Dual Solvent-Catalysts. *J. Am. Chem. Soc.* **2002**, *124*, 5962–5963.

(17) Xu, D.; Wu, J.; Luo, S.; Zhang, J.; Wu, J.; Du, X.; Xu, Z. Fischer indole synthesis catalyzed by novel SO_3H-functionalized ionic liquids in water. *Green Chem.* **2009**, *11*, 1239–1246.

(18) Leng, Y.; Wang, J.; Zhu, D.; Ren, X.; Ge, H.; Shen, L. Heteropolyanion-Based Ionic Liquids: Reaction-Induced Self-Separation Catalysts for Esterification. *Angew. Chem.* **2009**, *121*, 174–177.

(19) Yoshizawa, M.; Hirao, M.; Ito-Akita, K.; Ohno, H. Ion conduction in zwitterionic-type molten salts and their polymers. *J. Mater. Chem.* **2001**, *11*, 1057–1062.

(20) Yoshizawa, M.; Narita, A.; Ohno, H. Design of ionic liquids for Electrochemical Applications. *Aust. J. Chem.* **2004**, *57*, 139–144.

(21) Narita, A.; Shibayama, W.; Sakamoto, K.; Mizumo, T.; Matsumi, N.; Ohno, H. Lithium ion conduction in an organoborate zwitterion-LiTFSI mixture. *Chem Commun.* **2006**, 1926–1928.

(22) Kim, H.; Nguyen, D. Q.; Bae, H. W.; Lee, J. S.; Cho, B. W.; Kim, H. S.; Cheong, M.; Lee, H. Effect of ether group on the electrochemical stability of zwitterionic imidazolium compounds. *Electrochem. Commun.* **2008**, *10*, 1761–1764.

(23) Narita, C. A.; Shibayama, W.; Ohno, H. Structural factors to improve physico- chemical properties of zwitterions as ion conductive matrices. *J. Mater. Chem.* **2006**, *16*, 1475–1482.

(24) Tan, Z. C.; Sun, G. Y.; Sun, Y.; Yin, A. X.; Wang, W. B.; Ye, J. C.; Zhou, L. X. An adiabatic low-temperature calorimeterfor heat capacrry measurement of small samples. *J. Therm. Anal.* **1995**, *45*, 59–67.

(25) Tan, Z. C.; Sun, L. X.; Meng, S. H.; Li, L.; Xu, F.; Yu, P.; Liu, B. P.; Zhang, J. B. Heat capacities and thermodynamic functions of p-chlorobenzoic acid. *J. Chem. Thermodyn.* **2002**, *34*, 1417–1429.

(26) Tan, Z. C.; Shi, Q.; Liu, B. P.; Zhang, H. T. A fully automated adiabatic calorimeter for heat capacity measurement between 80 and 400 K. *J. Therm. Anal. Calorim.* **2008**, *92*, 367–374.
(27) Shi, Q.; Tan, Z. C.; Tong, B.; Di, Y. Y.; Zhang, Z. H.; Zeng, J. L.; Sun, L. X.; Li, Y. S. Low-temperature heat capacity and standard molar enthalpy of formation of crystalline 2-pyridinealdoxime ($C_6H_6N_2O$). *J. Chem. Thermodyn.* **2007**, *39*, 817–821.

Received for review April 26, 2010. Accepted August 17, 2010. This work was financially supported by the Knowledge Innovation Program of the Chinese Academy of Sciences Grant: DICP K2009D03 and the State Key Laboratory of Fine Chemicals (KF0811), Dalian University of Technology, China.

JE100423N